Long-term potentiation decay and memory loss are mediated by AMPAR endocytosis

Zhifang Dong,[1] Huili Han,[1] Hongjie Li,[1] Yanrui Bai,[1] Wei Wang,[1] Man Tu,[1] Yan Peng,[1] Limin Zhou,[1] Wenting He,[1] Xiaobin Wu,[1] Tao Tan,[1] Mingjing Liu,[1] Xiaoyan Wu,[1] Weihui Zhou,[1] Wuyang Jin,[2] Shu Zhang,[2,3] Todd Charlton Sacktor,[4] Tingyu Li,[1] Weihong Song,[1,5] and Yu Tian Wang[1,2,3]

[1]Ministry of Education Key Laboratory of Child Development and Disorders and Chongqing Key Laboratory of Translational Medical Research in Cognitive Development and Learning and Memory Disorders, Children's Hospital of Chongqing Medical University, Chongqing, China. [2]Brain Research Centre and Department of Medicine, University of British Columbia, Vancouver, British Columbia, Canada. [3]Graduate Institute of Immunology, China Medical University and Translational Medicine Research Center, China Medical University Hospital, Taichung, China. [4]Department of Physiology and Pharmacology and Department of Neurology, The Robert Furchgott Center for Neural and Behavioral Science, SUNY Downstate Medical Center, New York, New York, USA. [5]Brain Research Centre, Departments of Medicine and Psychiatry, University of British Columbia, Vancouver, British Columbia, Canada.

Long-term potentiation (LTP) of synaptic strength between hippocampal neurons is associated with learning and memory, and LTP dysfunction is thought to underlie memory loss. LTP can be temporally and mechanistically classified into decaying (early-phase) LTP and nondecaying (late-phase) LTP. While the nondecaying nature of LTP is thought to depend on protein synthesis and contribute to memory maintenance, little is known about the mechanisms and roles of decaying LTP. Here, we demonstrated that inhibiting endocytosis of postsynaptic α-amino-3-hydroxy-5-methyl-isoxazole-4-propionic acid receptors (AMPARs) prevents LTP decay, thereby converting it into nondecaying LTP. Conversely, restoration of AMPAR endocytosis by inhibiting protein kinase Mζ (PKMζ) converted nondecaying LTP into decaying LTP. Similarly, inhibition of AMPAR endocytosis prolonged memory retention in normal animals and reduced memory loss in a murine model of Alzheimer's disease. These results strongly suggest that an active process that involves AMPAR endocytosis mediates the decay of LTP and that inhibition of this process can prolong the longevity of LTP as well as memory under both physiological and pathological conditions.

Introduction

Activity-dependent long-term potentiation (LTP) of synaptic efficacy at the glutamatergic synapses in the hippocampus is the most well-characterized form of synaptic plasticity and has long been considered as a cellular mechanism underlying learning and memory (1–4). In support of the putative role of LTP in learning and memory, extensive work in in vivo animals has revealed a strong correlation between the maintenance of LTP and the maintenance of memory (5–7). Therefore, understanding the processes underlying LTP maintenance may in turn provide important information about the mechanisms of memory storage. LTP maintenance is often temporally and mechanistically divided into 2 phases, the decaying (or early) phase of LTP and the nondecaying (or late) phase of LTP (8, 9). Decaying LTP is often induced experimentally in brain slices and in vivo animals with a weak induction protocol (such as a single tetanic burst), can decay within hours, and does not depend on the synthesis of new protein(s). Conversely, nondecaying LTP can be induced with strong stimulation protocols (such as multiple tetani in quick succession), lasts hours and days, and may require new protein synthesis (10–13). Decaying LTP may be converted into nondecaying LTP, and such a con-

version is thought to be a critical process for the conversion of a short-term memory (STM) to a long-term memory (LTM) (14, 15). However, how and why decaying LTP decays in comparison with nondecaying LTP and how it can be converted into nondecaying LTP remain poorly understood.

Evidence accumulated in recent years supports the conjecture that the decay of LTP could be mediated by an active activity-dependent process, rather than a passive decay of processes required for maintaining LTP (16, 17). This leads us to hypothesize that this active process could be a feedback synaptic scaling mechanism. We speculate that, during decaying LTP, the increased synaptic efficacy may trigger an activity-dependent feedback synaptic downscaling mechanism that becomes functional, actively reducing the synaptic efficacy until LTP decays back to the basal level. We further reasoned that, during the production of nondecaying LTP, such a synaptic scaling mechanism becomes constantly inhibited by the newly synthesized molecule(s), so that the increased synaptic efficacy during nondecaying LTP is not scaled down. Thus, the tonic inhibition of such a putative negative feedback mechanism developed during decaying LTP by one or more newly synthesized proteins during nondecaying LTP is one of the critical steps for conversion of decaying LTP into nondecaying LTP.

Although the molecular substrate of such a putative synaptic scaling process remains unknown, Hou et al. and others have recently revealed that, in cultured hippocampal neurons,
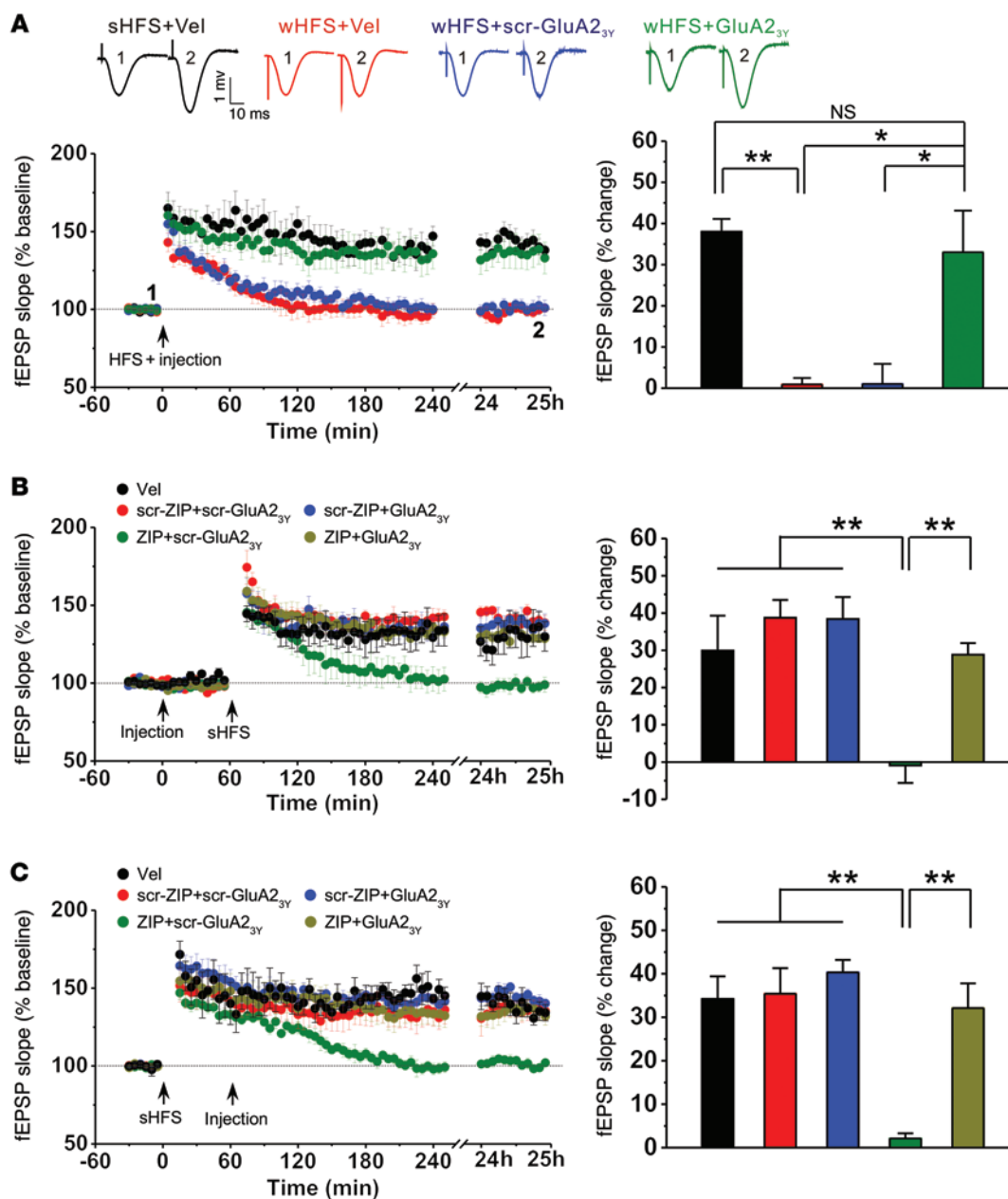
Figure 1. Active GluA2-dependent AMPAR endocytosis prevents the conversion of hippocampal CA1 decaying LTP into nondecaying LTP in freely moving rats. (**A**) Inhibition of GluA2-dependent AMPAR endocytosis converts decaying LTP into nondecaying LTP. The plot presents normalized slopes of fEPSPs; the bar graph summarizes the average percentage change of fEPSP slope immediately before (marked as 1) and 25 hours (marked as 2) after the induction, and corresponding representative traces are shown. wHFS (wHFS+Veh; $n = 5$) and sHFS (sHFS+Veh; $n = 5$) protocols reliably produce decaying LTP and nondecaying LTP, respectively. Application of Tat-GluA2$_{3Y}$ (wHSF+GluA2$_{3Y}$; $n = 7$), but not its control scr-GluA2$_{3Y}$ (wHFS+scr-GluA2$_{3Y}$; $n = 5$), prevented the decay of wHFS-induced LTP. (**B** and **C**) ZIP, applied either 1 hour (**B**) before or (**C**) after the induction stimulation, causes decay of sHFS-induced nondecaying LTP via GluA2-AMPAR endocytosis-dependent mechanism. The plot and bar graph show that ZIP peptide (ZIP+scr-GluA2$_{3Y}$; $n = 5$ for application either before or after sHFS) causes sHFS-induced nondecaying LTP to decay and this is prevented by coapplication of GluA2$_{3Y}$ (ZIP+ GluA2$_{3Y}$; $n = 6$ for application either before or after sHFS). The control scrambled ZIP has no observable effect in the presence of either GluA2$_{3Y}$ (scr-ZIP+GluA2$_{3Y}$; $n = 5$ for application either before or after sHFS) or its control (scr-ZIP+scr-GluA2$_{3Y}$; $n = 4$ and $n = 5$ for application before and after sHFS, respectively). *$P < 0.05$, **$P < 0.01$, Tukey's post-hoc analysis.

persistent enhancement of synaptic efficacy can trigger a synaptic input–specific homeostatic scaling mechanism that reduces the synaptic efficacy by endocytic removal of postsynaptic α-amino-3-hydroxy-5-methyl-isoxazole-4-propionic acid receptors (AMPARs) at these potentiated synapses (18, 19). Since decaying LTP is also a process involving persistent increase in synaptic

efficacy in a synaptic input–specific manner, we tested whether a similar activity-dependent AMPAR endocytosis process may function as a putative negative-feedback synaptic scaling mechanism responsible for the decay of LTP and, if so, whether pharmacological blockade of this process can convert decaying LTP into nondecaying LTP, thereby converting STM into LTM.
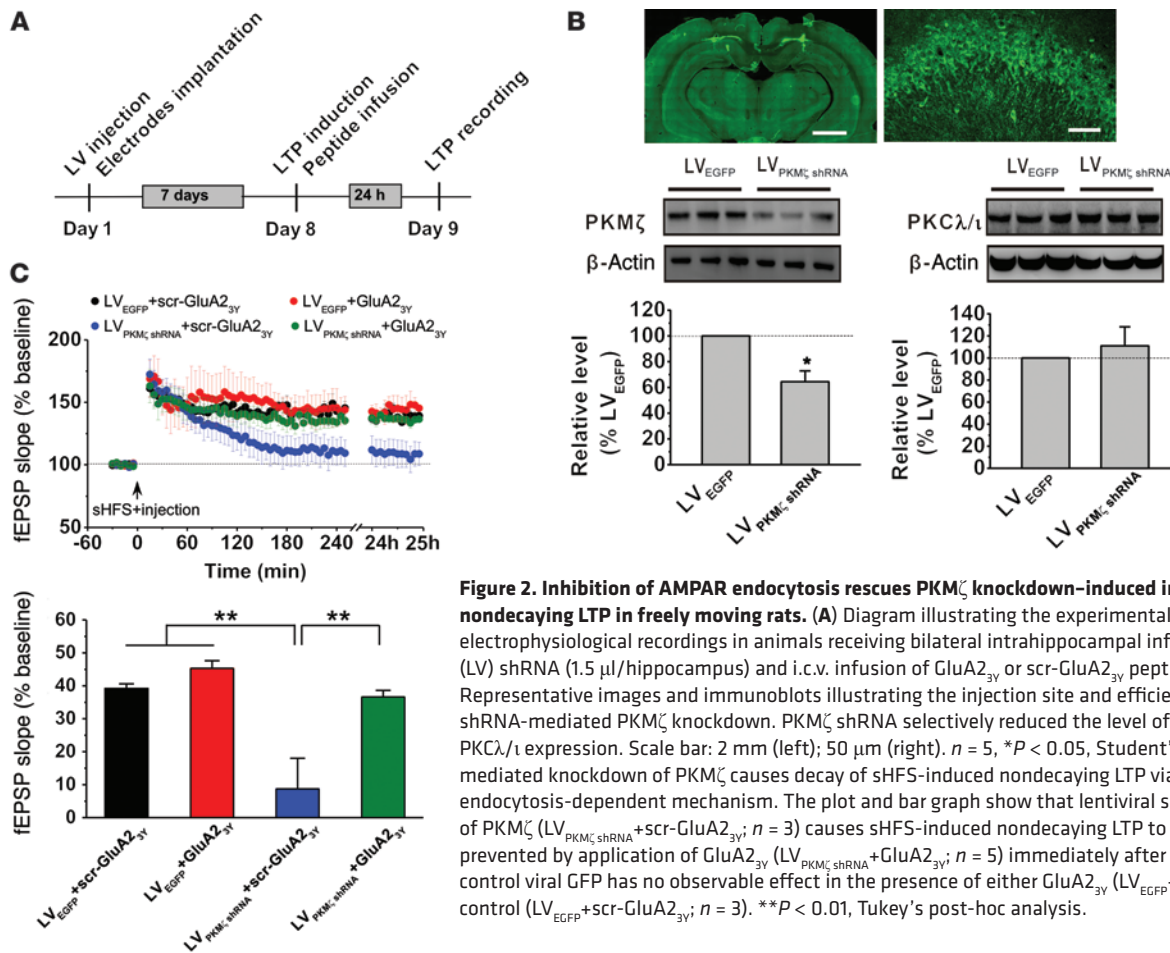
Figure 2. Inhibition of AMPAR endocytosis rescues PKMζ knockdown–induced impairment of nondecaying LTP in freely moving rats. (A) Diagram illustrating the experimental protocols for the electrophysiological recordings in animals receiving bilateral intrahippocampal infusions of lentiviral (LV) shRNA (1.5 μl/hippocampus) and i.c.v. infusion of GluA2$_{3Y}$ or scr-GluA2$_{3Y}$ peptide (500 pmol). **(B)** Representative images and immunoblots illustrating the injection site and efficiency of lentiviral shRNA-mediated PKMζ knockdown. PKMζ shRNA selectively reduced the level of PKMζ but not PKCλ/ι expression. Scale bar: 2 mm (left); 50 μm (right). $n = 5$, *$P < 0.05$, Student's t test. **(C)** shRNA-mediated knockdown of PKMζ causes decay of sHFS-induced nondecaying LTP via GluA2-AMPAR endocytosis-dependent mechanism. The plot and bar graph show that lentiviral shRNA knockdown of PKMζ (LV$_{PKMζ shRNA}$+scr-GluA2$_{3Y}$; $n = 3$) causes sHFS-induced nondecaying LTP to decay and this is prevented by application of GluA2$_{3Y}$ (LV$_{PKMζ shRNA}$+GluA2$_{3Y}$; $n = 5$) immediately after sHFS delivery. The control viral GFP has no observable effect in the presence of either GluA2$_{3Y}$ (LV$_{EGFP}$+ GluA2$_{3Y}$; $n = 5$) or its control (LV$_{EGFP}$+scr-GluA2$_{3Y}$; $n = 3$). **$P < 0.01$, Tukey's post-hoc analysis.

Results

Inhibition of AMPAR endocytosis converts decaying LTP into non-decaying LTP. In order to make the correlation of electrophysiological characterizations more relevant to behavioral analyses of memory maintenance, we studied both decaying LTP and nondecaying LTP using an in vivo model of hippocampal synaptic plasticity in freely moving adult rats (20, 21). Schaffer collateral stimulation-induced field excitatory postsynaptic potentials (fEPSPs) were recorded from the CA1 region. Electrical stimulation with a strong protocol of high-frequency stimulation (sHFS; 4 trains of 30 pulses at 100 Hz, with an intertrain interval of 5 minutes) reliably induced a characteristic nondecaying LTP of fEPSPs that lasted for more than 24 hours at least in vehicle control animals (sHFS+Vel; $n = 5$; 138.0% ± 3.1% at 25 hours after the induction; $P = 0.001$ vs. baseline; Figure 1A); whereas a weak high-frequency stimulation protocol (wHFS; 2 trains of 30 pulses at 100 Hz, with an intertrain interval of 5 minutes) was only able to induce a typical decaying LTP that decayed back to baseline level within 2 hours after the induction in vehicle control animals (wHFS+Vel; $n = 5$; 100.9% ± 1.8% at 25 hours after the induction; $P = 0.337$ vs. baseline, $P < 0.001$ vs. sHFS+Vel; Figure 1A).

To determine whether AMPAR endocytosis plays an essential role in mediating the decay of LTP, we used a well-characterized membrane-permeable GluA2-derived Tat-GluA2$_{3Y}$ peptide that has previously been shown to prevent activity-dependent AMPAR endocytosis, without affecting the constitutive AMPAR endocytosis and hence basal synaptic transmission in both brain slices in vitro (22–24) and freely moving animals in vivo (24–26). As expected, immediately following the induction of decaying LTP with wHFS, i.c.v. injections of Tat-GluA2$_{3Y}$ (GluA2$_{3Y}$; 500 pmol in 5 μl), but not its scrambled peptide (scr-GluA2$_{3Y}$) or saline vehicle control (Vel), significantly prolonged the maintenance of LTP, which remained at the potentiated level 24 hours after the induction (wHFS+scr-GluA2$_{3Y}$: $n = 5$, 101.0% ± 5.5%, $P = 0.911$ vs. baseline, $P = 0.992$ vs. wHFS+Vel; wHFS+GluA2$_{3Y}$: $n = 7$, 133.0% ± 10.9%, $P = 0.020$ vs. baseline, $P = 0.016$ vs. wHFS+Vel, $P = 0.017$ vs. wHFS+scr-GluA2$_{3Y}$, $P = 0.337$ Vs. sHFS+Vel; Figure 1A). Thus, inhibition of AMPAR endocytosis is sufficient to convert decaying LTP into nondecaying LTP. These results suggest that GluA2-dependent AMPAR endocytosis is a key process mediating the decay of LTP.

Next, we examined whether nondecaying LTP induced by sHFS is maintained by an active inhibition of this secondary (activity-dependent) AMPAR endocytosis. We reasoned that a process capable of producing nondecaying LTP (such as the sHFS used here), while producing LTP, can also trigger the translation-dependent synthesis of protein(s) that can actively suppress the secondary AMPAR endocytosis, thereby preventing LTP from decaying. Among many potential candidate molecules, we focused on the atypical PKC isoform, protein kinase Mζ (PKMζ), because its rapid translation has been suggested to have a critical role not only in the
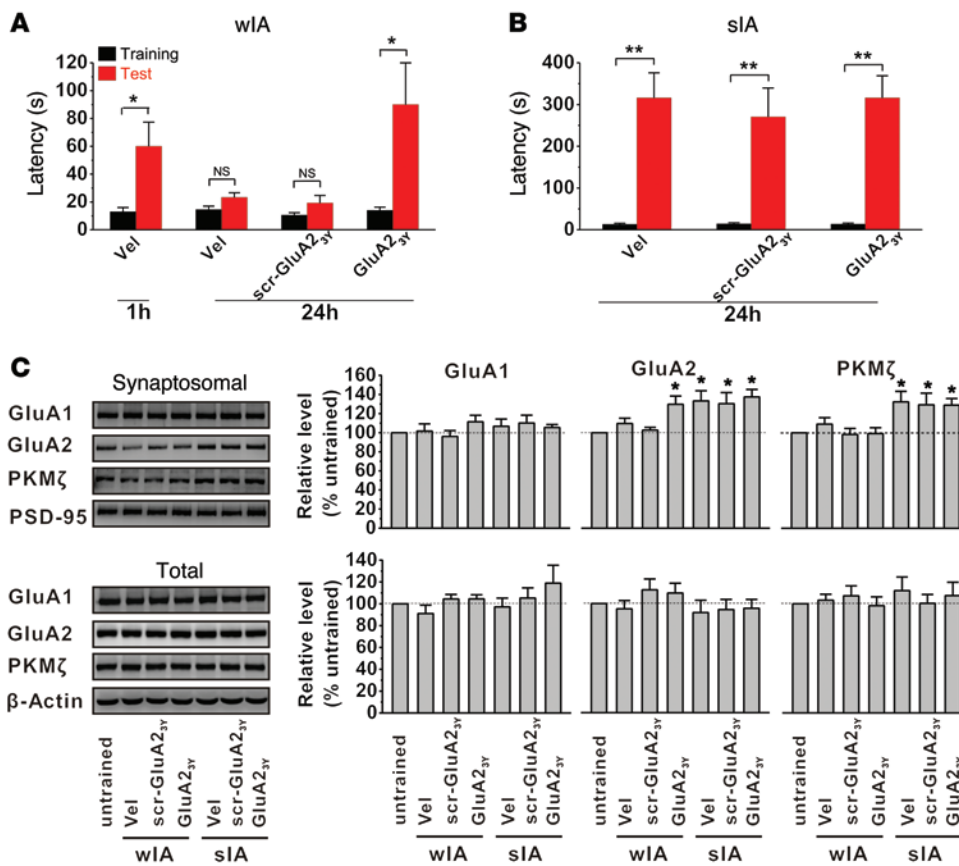
Figure 3. Blocking GluA2-dependent AMPAR endocytosis promotes LTM formation. (**A**) Inhibition of GluA2-dependent AMPAR endocytosis converts STM into LTM. wIA training produces only a STM that could be retrieved within 1 hour, but not at 24 hours, in control animals receiving bilateral intrahippocampal infusions of vehicle (*n* = 8 for either 1-hour or 24-hour test) immediately after training, however, this wIA training–induced STM is converted into a LTM that could be retrieved at 24 hours by bilateral intrahippocampal infusions of GluA2$_{3Y}$ (*n* = 12) but not its control (*n* = 11). (**B**) Inhibition of GluA2-dependent AMPAR endocytosis does not affect LTM formation. Neither GluA2$_{3Y}$ (*n* = 7) nor scr-GluA2$_{3Y}$ (*n* = 7) applied via bilateral intrahippocampal infusions show any effect on LTM formation induced by sIA training compared with vehicle (*n* = 12). (**C**) sIA training specifically increases synaptic GluA2 and PKMζ. Sequential immunoblotting of synaptosomal fraction and total tissue lysates of hippocampal tissues collected from animals in **A** and **B** immediately after memory was tested at 24 hours. wIA and sIA training differentially affect the levels of GluA2 and PKMζ in the synaptic fraction but not in total lysates. Note wIA training does not affect PKMζ and only increases the synaptic GluA2 level in rats treated with GluA2$_{3Y}$, whereas sIA training increases the levels of both PKMζ and GluA2 in the synaptic fraction. Neither wIA nor sIA has any effect on GluA1. *n* = 5, **P* < 0.05, ***P* < 0.01, Tukey's post-hoc analysis.

maintenance of LTP and memory (7) but also in regulating AMPAR trafficking (7, 26–28). We therefore tested whether sHFS-induced nondecaying LTP is maintained by the inhibition of AMPAR endocytosis by PKMζ with i.c.v. applications of PKMζ inhibitor ZIP (7) or its scrambled peptide (scr-ZIP), each at 25 nmol/5 μl in the absence or presence of GluA2$_{3Y}$ or its scrambled control peptide (500 pmol/5 μl), 1 hour prior to the induction of nondecaying LTP with sHFS (Figure 1B). Fluorescence imaging of hippocampal sections demonstrated a colocalization of FITC-ZIP and PSD-95 (a postsynaptic marker protein of excitatory synapses), and showed the successful diffusion of ZIP to hippocampal excitatory synapses, major sites of action for the peptide, 2 hours after i.c.v. administration of the peptide (Supplemental Figure 1; supplemental material available online with this article; doi:10.1172/JCI77888DS1). We reasoned that if PKMζ maintains nondecaying LTP by inhibiting the putative secondary AMPAR endocytosis, then inhibition of PKMζ with ZIP should release this active endocytosis process and thereby impair the maintenance of nondecaying LTP, converting it into a

decaying LTP. We further predicted that this ZIP effect should be prevented in the presence of GluA2$_{3Y}$. Supporting this line of reasoning, we found that, while sHFS reliably induced nondecaying LTP in the vehicle control group receiving the same volume of saline (Vel: *n* = 5, 129.9% ± 9.4%, *P* = 0.027 vs. baseline; Figure 1B), it only produced a decaying synaptic potentiation similar to that of decaying LTP in animals receiving a coapplication of ZIP and control scr-GluA2$_{3Y}$ (ZIP+scr-GluA2$_{3Y}$: *n* = 5, 99.1% ± 5.2%, *P* = 0.945 vs. baseline, *P* = 0.004 vs. Vel; Figure 1B), suggesting that ZIP is sufficient to prevent sHFS from inducing nondecaying LTP by converting it into decaying LTP. In contrast, application of GluA2$_{3Y}$ had little effect on the sHFS-induced nondecaying LTP on its own (scr-ZIP+GluA2$_{3Y}$: *n* = 5, 138.4% ± 6.6%, *P* = 0.006 vs. baseline, *P* = 0.376 vs. Vel; Figure 1B); this is not surprising, as AMPAR endocytosis may have been inhibited by PKMζ. However, when coapplied with ZIP, GluA2$_{3Y}$ prevented ZIP's ability to convert nondecaying LTP into decaying LTP (ZIP+GluA2$_{3Y}$: *n* =6, 128.8% ± 3.4%, *P* = 0.001 vs. baseline, *P* = 0.897 vs. Vel, *P* = 0.003 vs. ZIP+scr-
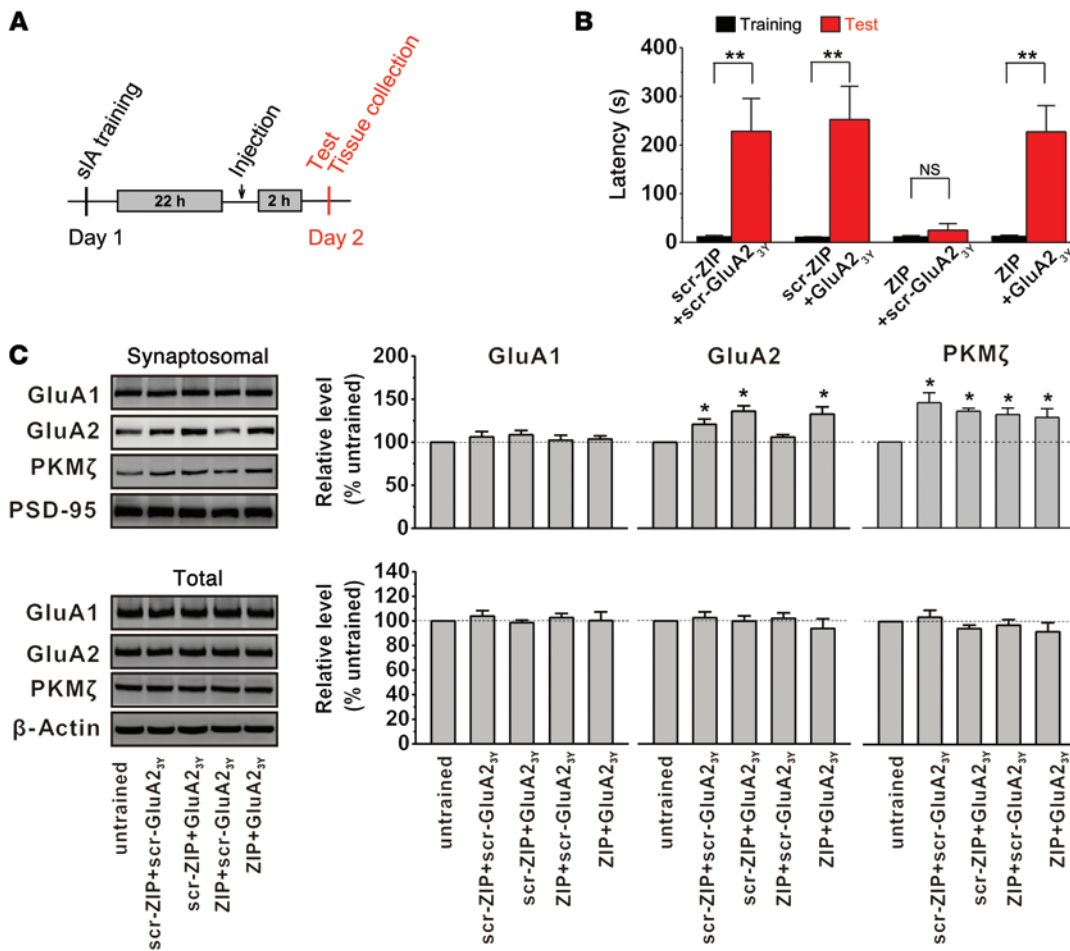
Figure 4. GluA2-dependent AMPAR endocytosis produced by PKMζ inactivation negatively regulates the memory retention. (**A**) Diagram illustrating the experimental protocols for sIA training and test (retrieval) and the times for bilateral intrahippocampal infusions of peptides. (**B**) Inhibition of GluA2-dependent AMPAR endocytosis rescues memory impairment induced by ZIP. ZIP (ZIP+scr-GluA2$_{3Y}$), but not its control scr-ZIP (scr-ZIP+scr-GluA2$_{3Y}$ or scr-ZIP+GluA2$_{3Y}$), impairs the sIA training–induced LTM, and this impairment is prevented by GluA2$_{3Y}$ (ZIP+GluA2$_{3Y}$). $n = 8$ in each group, **$P < 0.01$, Tukey's post-hoc analysis. (**C**) ZIP-induced memory impairment is associated with a specific reduction in synaptic GluA2 in the hippocampus. Sequential immunoblotting of synaptosomal fraction and total tissue lysates of hippocampal tissues collected from animals in **B** immediately after the memory tests. ZIP treatment specifically reduced synaptic GluA2, without affecting either GluA1 or PKMζ (ZIP+scr-GluA2$_{3Y}$). Coapplication of GluA2$_{3Y}$ prevented ZIP-induced reduction of GluA2, without affecting either GluA1 or PKMζ (ZIP+GluA2$_{3Y}$). $n = 5$, *$P < 0.05$, Tukey's post-hoc analysis.

GluA2$_{3Y}$; Figure 1B). In control experiments, we found that neither scr-ZIP nor scr-GluA2$_{3Y}$ affected sHFS-induced nondecaying LTP (scr-ZIP+scr-GluA2$_{3Y}$: $n = 4$, 138.7% ± 5.5%, $P = 0.005$ vs. baseline, $P = 0.386$ vs. Vel; Figure 1B). These results demonstrate that application of ZIP prior to the induction of nondecaying LTP was sufficient to prevent the maintenance phase of LTP through the release of inhibition on AMPAR endocytosis.

If nondecaying LTP is maintained by persistently inhibiting an active AMPAR endocytic process, we predict that ZIP should cause nondecaying LTP to decay, even when applied after the establishment of nondecaying LTP, and this effect should still be prevented by GluA2$_{3Y}$ application. When applied 1 hour after sHFS, ZIP (but not its control, scr-ZIP) was still capable of causing the sHFS-induced nondecaying LTP to gradually reduce to baseline within 2 hours of drug application (ZIP+scr-GluA2$_{3Y}$: $n = 5$, 102.1% ± 1.4%, $P = 0.573$ vs. baseline; Vel: $n = 4$, 134.3% ± 5.2%, $P = 0.019$ vs. baseline; scr-ZIP+scr-GluA2$_{3Y}$: $n = 5$, 135.4% ± 6.6%, $P = 0.008$

vs. baseline; scr-ZIP+GluA2$_{3Y}$: $n = 5$, 140.3% ± 3.2%, $P < 0.001$ vs. baseline; Figure 1C). Again, this effect of ZIP was prevented by the coapplication of GluA2$_{3Y}$ (ZIP+GluA2$_{3Y}$: $n = 6$, 132.1% ± 6.3%, $P = 0.004$ vs. baseline; Figure 1C).

The ability of ZIP to convert nondecaying LTP to decaying LTP and its prevention by GluA2$_{3Y}$ are all in a good agreement with our prediction that PKMζ is likely the newly translated molecule that inhibits the active AMPAR endocytosis during the maintenance of nondecaying LTP. However, the selectivity of ZIP as a PKMζ inhibitor has recently been challenged (29–31). To further confirm the involvement of PKMζ in this process, we used a lentivirus-mediated PKMζ shRNA to reduce PKMζ expression in the hippocampus (Figure 2). Western blots performed 7 days after a bilateral intrahippocampal infusion of viral particles showed that PKMζ shRNA (lentiviral PKMζ shRNA [LV$_{PKMζ shRNA}$], 1.5 μl per side) selectively reduced the level of PKMζ (LV$_{PKMζ shRNA}$, 64.4% ± 8.4% of lentiviral control [LV$_{EGFP}$], $P = 0.013$, $n = 5$ in each group; Figure 2B)
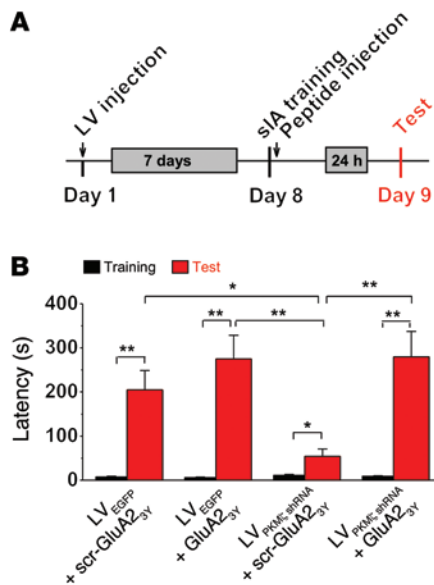
Figure 5. GluA2-dependent AMPAR endocytosis caused by PKMζ knockdown negatively regulates memory maintenance. (**A**) Diagram illustrating the experimental protocols for sIA training and test (retrieval), and the times for bilateral intrahippocampal infusions of lentivirus-mediated PKMζ shRNA (1.5 μl per side) and peptides. (**B**) Inhibition of GluA2-dependent AMPAR endocytosis rescues memory impairment induced by PKMζ knockdown. PKMζ shRNA (LV$_{PKMζ shRNA}$+scr-GluA2$_{3Y}$; n = 10), but not its control (LV$_{EGFP}$+scr-GluA2$_{3Y}$, n = 10 and LV$_{EGFP}$+GluA2$_{3Y}$, n = 13), impairs the sIA training–induced LTM, and this impairment is prevented by GluA2$_{3Y}$ (LV$_{PKMζ shRNA}$+GluA2$_{3Y}$, n = 12). *P < 0.05, **P < 0.01, Tukey's post-hoc analysis.

but not PKCλ/ι (LV$_{PKMζ shRNA}$, 105.1% ± 12.0% of LV$_{EGFP}$, P = 0.690, n = 5 in each group; Figure 2B) in the hippocampus. Consistent with the critical involvement of PKMζ in the inhibition of active AMPAR endocytosis, and hence the maintenance of nondecaying LTP, we found that 7 days after intrahippocampal infusion of PKMζ shRNA viral particles, shRNA-mediated PKMζ knockdown prevented sHFS from inducing nondecaying LTP, with the LTP being decayed back to baseline less than 2 hours after sHFS. This effect was prevented by GluA2$_{3Y}$ but not its control scr-GluA2$_{3Y}$ (500 pmol/5 μl, i.c.v.) delivered immediately after sHFS (LV$_{PKMζ shRNA}$+scr-GluA2$_{3Y}$: n = 5, 108.7% ± 9.3% at 25 hours after the induction, P = 0.456 vs. baseline, P = 0.006 vs. LV$_{EGFP}$+scr-GluA2$_{3Y}$, P = 0.002 vs. LV$_{EGFP}$+GluA2$_{3Y}$; LV$_{PKMζ shRNA}$+GluA2$_{3Y}$: n = 5, 136.6% ± 2.0% at 25 hours after the induction, P < 0.001 vs. baseline, P = 0.774 vs. LV$_{EGFP}$+scr-GluA2$_{3Y}$, P = 0.358 vs. LV$_{EGFP}$+GluA2$_{3Y}$, P = 0.004 vs. LV$_{PKMζ shRNA}$+scr-GluA2$_{3Y}$; Figure 2C). In contrast, a bilateral infusion of control viral particles had no obvious effect on the ability of sHFS to induce a nondecaying LTP in the presence of either GluA2$_{3Y}$ or its control scr-GluA2$_{3Y}$ (LV$_{EGFP}$+scr-GluA2$_{3Y}$: n = 3, 139.2% ± 1.4% at 25 hours after the induction, P = 0.002 vs. baseline; LV$_{EGFP}$+GluA2$_{3Y}$: n = 3, 145.3% ± 2.3% at 25 hours after the induction, P = 0.003 vs. baseline, P = 0.564 vs. LV$_{EGFP}$+scr-GluA2$_{3Y}$, Figure 2C).

Together, these results strongly suggest that PKMζ is likely the ZIP-sensitive molecule responsible for tonically inhibiting the secondary activity-dependent AMPAR endocytosis and thereby preventing LTP from decaying following sHFS.

Inhibition of AMPAR endocytosis converts STM into LTM. If maintenance of LTP is a critical cellular mechanism mediating memory storage, then converting decaying LTP into nondecaying LTP by inhibition of AMPAR endocytosis with GluA2$_{3Y}$ would be expected to convert STM into LTM. We first tested the physiological role of this conversion from decaying LTP to nondecaying LTP using a well-characterized hippocampus-dependent learning task, inhibitory avoidance (IA) training with a weak foot shock (wIA; 0.2 mA, 2 s) or with a strong foot shock (sIA; 0.4 mA, 2 s). Consistent with our recent report (20), wIA training could only produce STM

that could be retrieved within 1 hour (wIA-1h: n = 8, 59.8 ± 17.3 s for test, P = 0.014 vs. training) but not 24 hours (wIA-24h: n = 8, 23.3 ± 3.3 s for test, P = 0.084 vs. training; Figure 3A) following the training. As expected, bilateral intrahippocampal infusions of GluA2$_{3Y}$ (100 pmol per side in 1 μl) immediately after wIA training reliably and significantly promoted LTM formation so that memory could be retrieved 24 hours after training (GluA2$_{3Y}$: n = 12, 89.7 ± 29.7 s for test, P = 0.014 vs. training, P = 0.043 vs. Vel, P = 0.020 vs. scr-GluA2$_{3Y}$; Figure 3A). In control experiments, application of scr-GluA2$_{3Y}$ failed to prolong the memory retention (scr-GluA2$_{3Y}$: n = 11, 19.2 ± 5.5 s for test, P = 0.094 vs. training; Figure 3A). In contrast to wIA training, sIA training reliably produced LTM that could be recalled 24 hours after training. However, bilateral applications of either GluA2$_{3Y}$ or scr-GluA2$_{3Y}$ did not produce any notable effect on LTM formation induced by sIA training (Vel: n = 12, 315.9 ± 59.8 s for test, P = 0.001 vs. training; scr-GluA2$_{3Y}$: n = 7, 270.3 ± 69.4 s for test, P = 0.007 vs. training, P = 0.626 vs. Vel; GluA2$_{3Y}$: n = 7, 316.0 ± 53.0 s for test, P = 0.001 vs. training, P = 0.999 vs. Vel, P = 0.636 vs. scr-GluA2$_{3Y}$; Figure 3B).

These results strongly suggest that, as demonstrated in decaying LTP and nondecaying LTP, activity-dependent AMPAR endocytosis plays a critical role in constraining the ability of wIA training to produce LTM. Conversely, during formation of LTM by sIA training, as with the induction of nondecaying LTP with sHFS, AMPAR endocytosis may be inhibited by the increased amount and activity of a ZIP-sensitive molecule (such as PKMζ), and therefore application of endocytosis inhibitor GluA2$_{3Y}$ would have no effect on the LTM. We next investigated these predictions by directly measuring AMPAR synaptic localization and PKMζ expression in the hippocampi of animals subjected to either wIA or sIA training. We examined the expression levels of AMPAR subunits, along with PKMζ, in postsynaptic densities and total tissue lysates obtained 24 hours after training. Based on the above electrophysiological and behavioral results, we expected that wIA training may produce decaying LTP (as a result of increased function and/or numbers of synaptic AMPARs) but this would be gradually counteracted by a secondary activity-dependent increase in
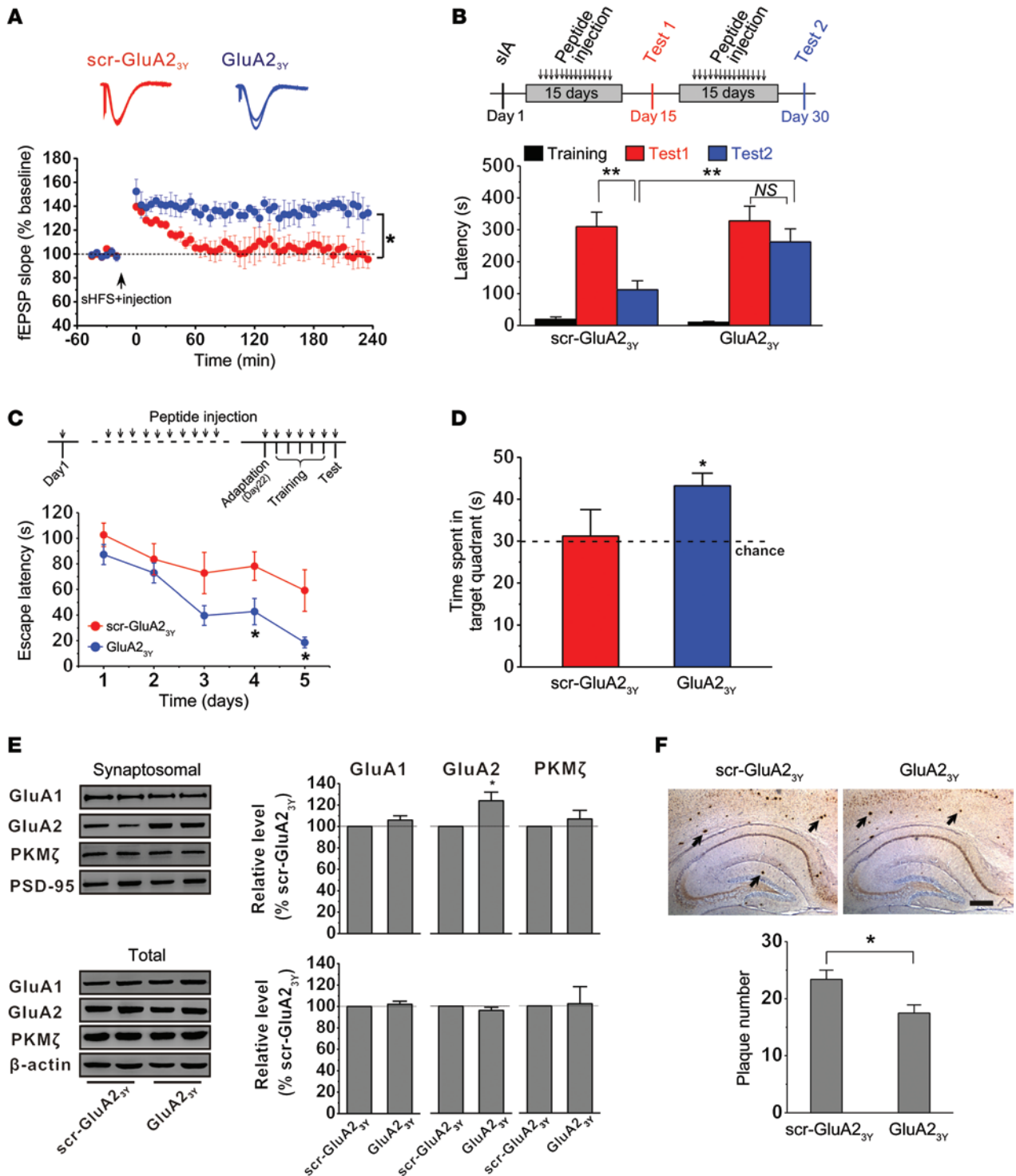
Figure 6. GluA2-dependent AMPAR endocytosis contributes to memory impairment in AD mice. (**A**) Inhibition of AMPAR endocytosis prevents the impairment of LTP maintenance in AD mice. The plot of fEPSP slope shows that sHFS is capable of inducing nondecaying LTP in mice receiving GluA2$_{3Y}$ but not control peptide. $n = 4$ in each group; *$P < 0.05$, Student's t test. (**B**) Inhibition of AMPAR endocytosis reduces impairment of memory maintenance in AD mice. IA tests show that LTM gradually decayed between 15 and 30 days and this memory impairment is fully rescued by chronic application of GluA2$_{3Y}$ ($n = 20$) but not its control ($n = 18$). **$P < 0.01$, Tukey's post-hoc analysis. (**C** and **D**) Inhibition of AMPAR endocytosis improves spatial learning and memory in water maze tests. Mice treated with GluA2$_{3Y}$ ($n = 7$) (**C**) spent less time finding the hidden platform on training day 4 and 5 and (**D**) spent much more time in the platform-located quadrant during probe testing compared with mice receiving scr-GluA2 ($n = 6$). Dashed line indicates the time in the platform-located quadrant by chance during probe testing. *$P < 0.05$, Tukey's post-hoc analysis. (**E**) The increase in synaptic GluA2 is critical for the improved memory maintenance in AD mice. GluA2$_{3Y}$, but not scr-GluA2$_{3Y}$, rescues the sIA training–induced increase in synaptic GluA2, without affecting the deficit in sIA training–induced synaptic localization of PKMζ. $n = 5$; *$P < 0.05$, Student's t test. (**F**) Chronic application of GluA2$_{3Y}$, but not scr-GluA$_{2Y}$, decreases neuritic plaque formation (arrows). Scale bar: 500 μm. $n = 12$ in each group; *$P < 0.05$, Student's t test.

AMPAR endocytosis at these potentiated synapses, leading to no net change in the total amount of synaptic AMPARs at the time point when LTM was recalled. In contrast, we expected that sIA training would result in an upregulation of ZIP-sensitive molecules, such as PKMζ, which in turn persistently inhibit decaying LTP-associated secondary AMPAR endocytosis, resulting in a persistent increase in the amount of synaptic AMPARs at the time of LTM recall. We found that a specific increase in the synaptic amount of GluA2 was only observed following sIA training, but not wIA training, and, more importantly, application of GluA2$_{3Y}$ (but not its control scr-GluA2$_{3Y}$) was able to increase the synaptic GluA2 amount following wIA training, similar to that after sIA training (Figure 3C; $n = 5$ in each group). However, localization of GluA1 (Figure 3C), GluA3 (Supplemental Figure 2A), and GluA4 (Supplemental Figure 2B) was not affected by wIA training– or sIA training–induced memory formation, suggesting that alteration of trafficking and expression of AMPARs containing these subunits may not play a critical role in IA tasks. These findings are consistent with a critical role of GluA2-containing AMPAR endocytosis in constraining wIA training to produce only STM. In agreement with our prediction that PKMζ is a ZIP-sensitive molecule, which inhibits secondary AMPAR endocytosis and thereby maintains LTM, we found that only sIA (but not wIA) training resulted in a significant increase in the level of PKMζ in synaptosomes, regardless of the presence or absence of GluA2$_{3Y}$ or scr-GluA2$_{3Y}$ (Figure 3C).

To test the causal role of PKMζ in inhibiting AMPAR endocytosis and, therefore, prolonging memory maintenance directly, we then examined whether inhibition of PKMζ by ZIP peptide applied 2 hours before LTM retrieval can disrupt sIA training–induced LTM and whether blockade of GluA2 endocytosis with GluA2$_{3Y}$ peptide at the same time can mimic PKMζ's function to inhibit AMPAR endocytosis, thereby preventing ZIP disruption of the sIA training–induced LTM (Figure 4A). In animals receiving bilateral intrahippocampal infusions of control peptides, sIA reliably induced LTM, which could be retrieved at 24 hours after the training (scr-ZIP+scr-GluA2$_{3Y}$: $n = 8$, 228.1 ± 67.6 s for test, $P = 0.011$ vs. training; scr-ZIP+GluA2$_{3Y}$: $n = 8$, 252.3 ± 68.5 s for test, $P = 0.007$ vs. training). However, this sIA training–induced LTM was significantly impaired by bilateral hippocampal administrations of ZIP (ZIP+scr-GluA2$_{3Y}$: $n = 8$, 25.1 ± 13.6 s for test, $P = 0.179$ vs. training; Figure 4B). As expected, the ZIP-induced impairment was prevented by coapplication of GluA2$_{3Y}$ (ZIP+ GluA2$_{3Y}$: $n = 8$, 227.0 ± 54.0 s for test, $P = 0.003$ vs. training; Figure 4B). These results support our prediction that PKMζ maintains memory retention by inhibition of GluA2 AMPAR endocytosis, while ZIP impairs memory retention by disrupting this mechanism.

Consistent with these behavioral results, 24 hours after training, immunoblot analysis of synaptosomal (synaptic) and lysate (total) amounts of PKMζ and AMPARs in hippocampal tissues ($n = 5$ in each group) revealed a marked increase in postsynaptic expression of PKMζ in all groups of animals that received sIA training relative to levels seen in untrained control groups. In comparison, the amount of synaptic GluA2 (but not GluA1) was also increased in all training groups except for the ZIP-treated group (ZIP+scr-GluA2$_{3Y}$; Figure 4C). It is important to point out that the ZIP-treated group was also the only group in which LTM was impaired (Figure 4B). Moreover, this inhibition of sIA training–induced increase in syn-

aptic GluA2 AMPARs by ZIP was prevented by coapplication of GluA2$_{3Y}$ (Zip+GluA2$_{3Y}$; Figure 4C). Notably, there was no difference in the total levels of PKMζ, GluA2, and GluA1 among all these groups (Figure 4C). Thus, similar to the mechanisms involved in the conversion of decaying LTP to nondecaying LTP, our results strongly support the notion that GluA2 endocytosis is a critical determinant for constraining memory retention, with a ZIP-sensitive molecule, likely PKMζ maintaining memory retention by constantly inhibiting this memory-constraining mechanism.

To further confirm that sIA training–induced increase in synaptic PKMζ inhibits a secondary AMPAR endocytosis, thereby ensuring the formation of inhibition, we next compared the longevity of sIA training–induced memory between animals that received bilateral intrahippocampal infusions of control or PKMζ shRNA viral particles (1.5 μl per side) 7 days prior to the training (Figure 5A). sIA training reliably induced LTM that could be retrieved after 24 hours in animals receiving control viral particles, and this was not affected by an immediate intrahippocampal infusion (100 pmol per side in 1 μl) of either GluA2$_{3Y}$ or scr-GluA2$_{3Y}$ peptide after sIA training (LV$_{EGFP}$+scr-GluA2$_{3Y}$: $n = 10$, 203.5 ± 44.0 s for retrieval test, $P = 0.001$ vs. training; LV$_{EGFP}$+GluA2$_{3Y}$: $n = 13$, 274.7 ± 53.8 s for test, $P < 0.001$ vs. training, $P = 0.312$ vs. LV$_{EGFP}$+scr-GluA2$_{3Y}$, Figure 5B). However, the ability of sIA training to induce LTM was significantly impaired in animals receiving PKMζ shRNA viral particles (LV$_{PKMζ\ shRNA}$+scr-GluA2$_{3Y}$: $n = 10$, 54.1 ± 16.8 s for test, $P = 0.031$ vs. training, $P = 0.046$ vs. LV$_{EGFP}$+scr-GluA2$_{3Y}$, $P = 0.003$ vs. LV$_{EGFP}$+GluA2$_{3Y}$; Figure 5B). As expected, the impairment induced by shRNA-mediated PKMζ knockdown was prevented by the bilateral intrahippocampal infusion of GluA2$_{3Y}$ immediately after sIA training (LV$_{PKMζ\ shRNA}$+GluA2$_{3Y}$: $n = 12$, 279.6 ± 57.7 s for test, $P = 0.001$ vs. training, $P = 0.289$ vs. LV$_{EGFP}$+scr-GluA2$_{3Y}$, $P = 0.941$ vs. LV$_{EGFP}$+GluA2$_{3Y}$, $P = 0.002$ vs. LV$_{PKMζ\ shRNA}$+scr-GluA2$_{3Y}$; Figure 5B). These results are in full agreement with the aforementioned results with ZIP and thereby further confirm that PKMζ maintains LTM by inhibition of the secondary GluA2-dependent AMPAR endocytosis.

Inhibition of AMPAR endocytosis reduces memory loss in a transgenic mouse model of Alzheimer's disease. Alzheimer's disease (AD), one of the most common neurodegenerative diseases leading to dementia, is characterized by progressive memory loss and other cognitive dysfunctions, due, at least in part, to the impairment of synaptic plasticity (32, 33). Indeed, recent work has reported evidence for postsynaptic degeneration and mislocalization of PKMζ to neurofibrillary tangles in brain structures of patients with AD important for memory formation, including the hippocampus (34, 35). Given the important role of PKMζ-mediated inhibition of GluA2 AMPAR endocytosis in maintaining LTP and memory retention, we hypothesize that dysfunction of PKMζ-mediated inhibition of GluA2 AMPAR endocytosis, due to mislocalization or failure to increase PKMζ expression in AD, may prevent the increase in synaptic GluA2 levels during the maintenance of LTP and memory, thereby contributing to the impairment of LTP and memory dysfunction observed in AD. If so, we further reasoned that inhibition of AMPAR endocytosis using the GluA2$_{3Y}$ peptide may reduce the impairment of nondecaying LTP and LTM in AD. We tested this hypothesis using a well-characterized AD model of APP23/PS45 double-trans-

genic mice (referred to herein as AD mice) (36, 37). As shown in Figure 6A, fEPSP recordings in vivo revealed that sHFS could only induce a decaying LTP that lasted for less than 1 hour in AD mice (aged 2.5 months) receiving control peptide infusion (scr-GluA2$_{3Y}$, 3 μmol/kg, i.p.) 1 hour prior to sHFS (scr-GluA2$_{3Y}$: 95.5% ± 7.4% at 4 hours after sHFS; n = 4, P = 0.754 vs. baseline before sHFS). This suggests a severe impairment in LTP maintenance in these mice. However, application of GluA2$_{3Y}$ (3 μmol/kg, i.p.) prevented the rundown of LTP, converting this decaying LTP into nondecaying LTP (GluA2$_{3Y}$: 134.4% ± 5.9% at 4 hours after sHFS; n = 4, P = 0.016 vs. baseline, P = 0.013 vs. scr-GluA2$_{3Y}$; Figure 6A). Next, we examined the ability of GluA2$_{3Y}$ to reduce memory impairment in these AD mice. As shown in Figure 6B, we first trained the animals (aged 1.5 months) using an IA task with a strong intensity foot shock (1.5 mA, 2 s) in order to establish a stable IA memory trace for the task in these mice. After a single IA training, animals were subjected to systemic injection of GluA2$_{3Y}$ or scr-GluA2$_{3Y}$ (3 μmol/kg, i.p.) daily for 30 days. Two retrieval tests were performed at day 15 and day 30 after IA training to determine LTM retention. The retrieval test at day 15 (test 1; Figure 6B) revealed that, regardless of the treatments, all animals showed stable memory retention for the IA tasks, as evidenced by the similar avoidance latency between animals administered GluA2$_{3Y}$ and those administered scr-GluA2$_{3Y}$ (scr-GluA2$_{3Y}$: n = 18, 298.1 ± 44.3 s for test, P = 0.001 vs. training; GluA2$_{3Y}$: n = 20, 327.8 ± 45.9 s for test, P = 0.001 vs. training, P = 0.332 vs. scr-GluA2$_{3Y}$; test 1; Figure 6B). This suggests that the LTM was established by the training protocol in these animals and that, at this point in time, the cognitive ability in these animals was not significantly affected. In contrast, by day 30, animals receiving the control scr-GluA2$_{3Y}$ peptide treatment showed a significantly shortened avoidance latency when compared with that observed in animals treated with GluA2$_{3Y}$ (scr-GluA2$_{3Y}$: n = 18, 111.7 ± 27.9 s for test, P = 0.003 vs. training; GluA2$_{3Y}$: n = 20, 261.5 ± 40.9 s for test, P = 0.001 vs. training, P = 0.004 vs. scr-GluA2$_{3Y}$; test 2; Figure 6B). These results strongly suggest that there is a significantly impaired cognitive function in these animals (as exemplified by the reduced memory retention) and that this memory decay process can be significantly inhibited by treatment with GluA2$_{3Y}$.

In order to further evaluate the effect of GluA2$_{3Y}$ on amelioration of memory deficits in these AD mice, we performed another hippocampus-dependent learning and memory task, the Morris water maze task. After daily GluA2$_{3Y}$ (n = 7, 3 μmol/kg, i.p.) or scr-GluA2$_{3Y}$ (n = 6, 3 μmol/kg, i.p.) treatment for 3 weeks, mice (aged 1.5 months) were subjected to water maze training for 5 days and a probe test on day 6. The results showed that GluA2$_{3Y}$ treatment dramatically shortened the escape latency for searching for the hidden platform on training day 4 (scr-GluA2$_{3Y}$: 78.2 ± 11.2 s; vs. GluA2$_{3Y}$: 42.8 ± 10.3 s; P = 0.046; Figure 6C) and 5 (scr-GluA2$_{3Y}$: 59.2 ± 16.2 s; vs. GluA2$_{3Y}$: 18.6 ± 4.2 s; P = 0.033; Figure 6C) relative to scr-GluA2$_{3Y}$ controls. Furthermore, the probe test data also showed that mice treated with GluA2$_{3Y}$ spent much more time in the hidden platform quadrant on day 6 compared with mice treated with scr-GluA2$_{3Y}$ (scr-GluA2$_{3Y}$: 319.2 ± 6.2 s; vs. GluA2$_{3Y}$: 43.2 ± 3.0 s; P = 0.025; Figure 6D). These results further suggest that the inhibition of AMPAR endocytosis by GluA2$_{3Y}$ treatment significantly slows down the memory decline in AD mice.

To correlate electrophysiological and behavioral cognitive changes with biochemical alterations of synaptic GluA2 and PKMζ, we performed immunoblotting of hippocampal synaptosomal fractionations and total tissue lysates from these animals immediately after the second IA retrieval test. As shown in Figure 6E (n = 5 in each group), we found that these AD mice treated with GluA2$_{3Y}$ showed a significant increase in synaptic GluA2, but not synaptic GluA1 or PKMζ, when compared with mice treated with control peptide (scr-GluA2$_{3Y}$). Neither treatment affected the total levels of GluA1, GluA2, or PKMζ (Figure 6E). Our results are consistent with the notion that under nontreated conditions sHFS or sIA training in AD fails to cause a translocation of PKMζ to the synapse, possibly due to its mislocalization into neurofibrillary tangles (34, 35). This in turn results in uninhibited secondary AMPAR endocytosis, leading to the failure to increase synaptic GluA2. These conjectures can further explain why the application of GluA2$_{3Y}$ alone is able to rescue the LTP maintenance and reduce memory impairment in AD, as it can prevent this secondary AMPAR endocytosis without the need for an increase in synaptic PKMζ.

Neuritic plaques represent one of the main histopathological hallmarks in AD brains and are thought to play a critical role in mediating the excitotoxicity responsible for AD neuronal damage, including the loss of both synapses and neurons (38–40). In turn, this excitotoxicity further facilitates the formation of neuritic plaques (41). It is interesting to note that, in one of our previous studies, we observed that facilitated GluA2-dependent AMPAR endocytosis is associated with neuronal apoptosis produced by excitotoxicity and, more importantly, that blocking this AMPAR endocytosis with GluA2$_{3Y}$ can prevent this excitotoxicity-induced neuronal apoptosis (42). Others have also reported that facilitated GluA2 endocytosis is in fact sufficient and necessary to mediate Aβ-mediated neuronal injuries (43). Therefore, we suspect that our chronic applications of GluA2$_{3Y}$ peptide in AD mice, through reducing excitotoxicity, may also decrease neuritic plaque formation in these animals. To test this prediction, brains from these GluA2$_{3Y}$- and scr-GluA2$_{3Y}$–treated AD mice were processed and examined for Aβ-containing neuritic plaques using 4G8 immunostaining. Neuritic plaque formation was significantly decreased in AD mice treated with GluA2$_{3Y}$ in comparison with that in mice treated with control peptide (scr-GluA2$_{3Y}$: 23.4 ± 1.6 plaques; GluA2$_{3Y}$: 17.5 ± 1.4 plaques; n = 12 in each group; P = 0.011; Figure 6F).

Discussion

Previous studies have suggested that the decay of LTP is not mediated by a passively gradual rundown of a LTP-maintaining mechanism but as a result of active inhibition. Here, we present results that not only further support this view but also strongly indicate that this tonic inhibition of LTP maintenance is at least in part mediated by a mechanism involving GluA2-dependent AMPAR endocytosis. As blockade of this AMPAR endocytosis has no effect on either basal synaptic transmission or the induction of LTP, our results support the notion that this AMPAR endocytosis may represent a feedback mechanism secondary to the increased synaptic efficacy during LTP. Although the mechanisms by which increased synaptic efficacy activates such a secondary AMPAR endocytosis are still unclear, Hou et al. and others have recently reported a novel input-specific homeostatic downregulation of synaptic

efficacy mediated by increased endocytosis and consequent degradation of postsynaptic AMPARs (18, 19). This may suggest that the activity-dependent homeostasis revealed by Hou et al. and the feedback GluA2-dependent AMPAR endocytosis demonstrated in this work may share certain common mechanistic steps.

In addition to the active contribution of the GluA2-dependent AMPAR endocytosis to the decay of LTP, its inhibition also appears critical for the maintenance of nondecaying LTP; this was supported by our observations that ZIP is capable of causing decay of LTP and by the evidence that this ZIP effect can be prevented by blocking AMPAR endocytosis. Thus, this AMPAR endocytosis feedback mechanism appears active not only during decaying LTP but throughout the maintenance phase of nondecaying LTP. The nondecaying characteristic of LTP seems to be due to an active inhibition of such a tonically active process by a ZIP-sensitive molecular mechanism. We favor PKMζ, among the potential candidates, as the ZIP target(s) that inhibits GluA2-dependent endocytosis for several reasons. First, PKMζ can be rapidly and persistently induced during and required for the maintenance of LTP and memory (7, 26–28). Second, existing evidence strongly suggests that PKMζ maintains nondecaying LTP in slice preparations, at least in part, by altering GluA2 trafficking (28). Third, in this study we were able to demonstrate that the increase in synaptic PKMζ is specifically associated with the sHFS-induced nondecaying LTP and sIA training–induced LTM formation but not wHSF-induced decaying LTP or wIA training–induced STM. Fourth, we showed that shRNA-mediated PKMζ knockdown mimicked ZIP, thereby impairing the maintenance of both nondecaying LTP and LTM. Finally, and most significantly, we directly demonstrated that the impairment by PKMζ knockdown was indeed mediated by its action of inhibiting GluA2-dependent endocytosis, as this effect was fully prevented (or occluded) by GluA2$_{3Y}$. However, it should also be pointed out that the absolute requirement of PKMζ in the maintenance of LTP as well as LTM has recently been challenged (29–31) and that ZIP appears to also inhibit protein kinase isoforms other than PKMζ (44). Thus, it may remain possible that a ZIP-sensitive molecule other than PKMζ may be involved in mediating the inhibition of this secondary GluA2-dependent AMPAR endocytosis, thereby maintaining both nondecaying LTP and LTM.

Although the role of activity-dependent synaptic plasticity such as LTP in memory maintenance remains to be established, this notion is supported by a large body of correlative evidence (1–4). Our results demonstrating that the blockade of AMPAR endocytosis is similarly capable of converting decaying LTP to nondecaying LTP, and STM into LTM, reflect the critical role of decaying LTP and nondecaying LTP in mediating STM and LTM, respectively. In addition, our study identifies the endocytosis of GluA2-containing AMPARs as the common and critical step in constraining the conversion of decaying LTP to nondecaying LTP and of STM to LTM. Thus, our work provides strong evidence for a critical role of GluA2-dependent endocytosis, and hence the synaptic density of GluA2 subunits, in determining the longevity of LTP and memory. It is interesting to note that the increased synaptic GluA2 subunits observed during either nondecaying LTP or LTM was not associated with any notable change in other AMPAR subunits, including the GluA1 subunit. This is somewhat surprising given that an increased synaptic insertion of GluA1 homomeric AMPARs has previously been suggested to be important for both LTP expression (2, 45) and learning/memory (46, 47). However, as the increased synaptic insertion of GluA1 homomeric AMPARs is likely a transient phenomenon, only occurring within minutes after the induction of LTP (45, 48), such an increase in synaptic insertion of GluA1 homomeric AMPARs would have been replaced by an increase in GluA2-containing and GluA1-lacking (likely GluA2 homomeric) AMPARs during nondecaying LTP and LTM when these subunits were analyzed in Western blots.

If endocytosis of AMPARs has a critical role in causing LTP decay, an abnormal increase in this process could contribute to the impairment of LTP maintenance and memory retention associated with some cognitive disorders. The fact that GluA2$_{3Y}$ can rescue LTP impairment and slow the progressive memory loss in the transgenic AD mice described here supports this view. However, it is somewhat surprising that in this work we also observed a significant effect of GluA2$_{3Y}$ in reducing excitotoxic neuritic plaques in these AD mice. Since no increase in GluA1 homomeric AMPARs was observed following sIA training–induced memory under either physiological or pathological conditions, a critical contribution to this excitotoxic AD pathology from an increase in Ca^{2+}-permeable GluA1 homomeric AMPARs is unlikely. In this regard, it is interesting to note that, in one of our previous studies, we observed that facilitated GluA2-dependent AMPAR endocytosis is associated with neuronal apoptosis produced by NMDA and ischemia-induced excitotoxicity and, more importantly, that blocking this AMPAR endocytosis with the GluA2$_{3Y}$ peptide can prevent this excitotoxicity-induced neuronal apoptosis (42). Others have reported that facilitated GluA2 endocytosis is in fact sufficient and necessary to mediate Aβ-mediated neuronal injuries (43). Thus, our results here, along with those from recent studies (42), strongly suggest that GluA2-dependent AMPAR endocytosis may represent an essential step in mediating certain forms of neuronal excitotoxicity. While how AMPAR endocytosis mediates excitotoxic neuronal death remains unclear, we have recently demonstrated that AMPAR endocytosis-induced neuronal death appears to be mediated by both enhancing the caspase-3 death-signaling pathway and inhibiting the PI3K survival-signaling pathway (42). Interestingly enough, Li and colleagues (49) have also recently reported that caspase-3 activation via mitochondria is actually required for AMPAR endocytosis and hence the expression of long-term depression. Together, these studies suggest that there may be a positive feedback interplay between AMPAR endocytosis and caspase-3 in mediating excitotoxic neuronal death. In this scenario, by preventing GluA2-dependent endocytosis, the GluA2$_{3Y}$ peptide can be expected to disrupt this self-amplified excitotoxic death signaling, thereby reducing excitotoxic neuritic plaques in AD mice. Thus, our results shown here that GluA2$_{3Y}$ not only rescues LTP impairment and slows memory loss but also reduces excitotoxic neuritic plaques in transgenic AD mice provide scientific basis for the development of AMPAR endocytosis blockers, such as GluA2$_{3Y}$, as potential therapeutics for treating the learning and memory deficits associated with both patients with AD and aged populations.

Methods

Animals

Adult male Sprague-Dawley rats (300–350 g, aged 8–10 weeks) and transgenic mice (aged 1.5 months) were housed in plastic cages in a temperature-controlled (21°C) colony room on a 12-hour light/12-hour dark cycle, and all electrophysiological and behavioral experiments were conducted during light cycle. Food and water were available ad libitum. APP23 transgenic mice carry human APP751 cDNA with the Swedish double mutation at positions 670/671 (KM → NL) under control of the murine Thy-1.2 expression cassette. PS45 transgenic mice carry human presenilin-1 cDNA with the M146V mutation. The genotype of the mice was confirmed by PCR using DNA from tail tissues.

Peptides and antibodies

The AMPAR endocytosis inhibitor Tat-GluA2$_{3Y}$ (YGRKKRRQRRR-YKEGYNVYG), scrambled Tat-GluA2$_{3Y}$ (YGRKKRRQRRR-VYKY-GGYNE), the PKMζ inhibitor ZIP (myr-SIYRRGARRWRKL-OH), scrambled ZIP (myr-RLYRKRIWRSAGR-OH), and FITC-ZIP peptides were synthesized by GL Biochem Ltd. All peptides were dissolved in 0.9% sterile saline at required concentrations.

Mouse anti–Aβ monoclonal antibody was obtained from Signet Laboratories (SIG-39240). Mouse anti-GluA2 (MAB397) and anti–PSD-95 (MAB1598) monoclonal antibodies were obtained from Millipore. Rabbit anti-GluA1 (AB312320), anti-PKMζ (AB59364), and anti–β-actin (AB8227) polyclonal antibodies were purchased from Abcam. Rabbit anti-PKCλ/ι (C83H11) monoclonal antibody was from cell signaling.

Lentiviral shRNA-mediated knockdown of hippocampal PKMζ

To reduce the expression of PKMζ, we used a lentivirus-mediated PKMζ small hairpin RNA (shRNA), which was constructed by Genomeditech Ltd. The siRNA sequence targeting rat PKMζ, 5′-GCAAGCTGCTTGTCCATAAAC-3′, has been shown previously to efficiently downregulate rat PKMζ expression (50). Pairs of complementary oligonucleotides containing these sequences were synthesized and cloned into the pGMLV-SB1 lentivector. The pGMLV-SB1 lentivectors containing the shRNA sequences were transfected into 293T producer cells. Viral supernatants were harvested after 48 hours, and the titers were determined with serial dilutions of concentrated lentivirus. Titers were 3×10^9 TU/ml.

Bilateral hippocampal microinjection

Surgery. One hundred and fifty rats were chronically implanted with cannulas above dorsal hippocampi as previously described (20), and 8 animals were excluded from the experiment due to nonfunctional cannulas or postoperative complications. Briefly, rats were anesthetized with sodium pentobarbital (60 mg/kg, i.p.). Atropine (0.4 mg/kg, i.p.) was also given to help relieve respiratory congestion. Scalp skin was shaved with clippers and disinfected using iodine before rats were mounted on a stereotaxic instrument. After opening the scalp skin and exposing the skull, two 22-gauge stainless steel guide cannulas (10 mm; Plastics One Inc.) were implanted above the dorsal hippocampi (3.5 mm posterior to bregma, 2.5 mm lateral to the midline, and 2.5 mm below the surface of the dura) and fixed to the skull with 4 jeweler's screws and dental cement. Sterile dummy cannula (30-gauge stainless steel rod, 10 mm in length; Plastics One Inc.) were inserted into guide cannula to avoid bacterial infection and cerebral spinal fluid leakage through the cannula. All rats were allowed to recover for 7 to 10 days before experiments.

Habituation. On the day prior to experiments, the animals were placed in the experiment room and given a sham intrahippocampal injection to become acclimatized to the injection procedure. Dummy cannulas were removed, and the rats were placed into a Plexiglas injection box (25 × 45 × 25 cm, same as home cage), with 30-gauge injection cannulas in their guide cannulas. Injection cannulas (11 mm; Plastics One Inc.) were connected to a microsyringe pump (Harvard Apparatus) by PE-50 tubing, which was 1 mm beyond the tip of the guide cannulas.

Intrahippocampal microinjection. Drugs were injected with 10 μl Hamilton syringes and a microsyringe pump at 0.5 μl/min for 2 minutes. After injection, the injection cannulas were left in place for an additional minute to allow for the diffusion of the drug away from the cannula tips. The rats were then removed from the injection box, their dummy cannulas replaced, and they were placed back in their home cages.

IA task

Apparatus. The IA apparatus is a 2-chambered Perspex box consisting of a lighted safe compartment separated by an automatic trap door from a dark shock compartment (25 × 20 × 20 cm for each compartment; San Diego Instruments Inc.).

Procedures. One day before training, animals were allowed to freely explore both chambers for 3 minutes. On the training day, animals were placed in the safe compartment facing a corner opposite the door. Ten seconds later, the trap door was opened to allow the animals to enter the dark compartment. After the animals entered the dark compartment, the door was closed and they received a foot shock via electrified steel grids on the box floor (28 grids at the intergrid interval of 1.8 cm for rats, 62 grids at the intergrid interval of 0.8 cm for mice). In this study, 2 intensity foot shocks for rat experiments were used: (a) a wIA training (0.2 mA, 2 s) and (b) a sIA training (0.4 mA, 2 s) to produce STM (1 hour after training) and LTM (24 hours after training), respectively. For transgenic mouse experiments, a stronger foot shock (1.5 mA, 2 s) was used to produce a solid LTM that could last for over 15 days. After IA training, the animals were given 15 seconds to recover in the dark compartment before being returned to their home cages. The animals were submitted to a test session to measure STM or LTM. Memory was assessed by placing trained animals back in the lighted compartment of the box and measuring latencies for the animals to reenter the dark compartment. Reentry was counted when all of the animal's 4 paws were back in the dark compartment of the box. No foot shock was administered during retention assays, and measurements were terminated at a ceiling test latency of 540 s.

Water maze task

The Morris water maze consisted of a circular stainless steel pool (150 cm in diameter) filled with water (25°C ± 1°C) made opaque with nontoxic white paint. The pool was surrounded by light blue curtains, and 3 distal visual cues were fixed to the curtains. A CCD camera suspended above the pool center recorded the swim paths of the animals, and video output was digitized by an Any-maze tracking system (Stoelting). The pool was artificially divided into 4 quadrants: NE, NW, SW, and SE. The Morris water maze test includes spatial training and probe test. Twenty-four hours before spatial training, the animals were

allowed to adapt to the maze for a 120-second free swim. The animals were then trained in the spatial learning task for 6 trials per day for 5 consecutive days. In each trial, mice were placed into water from 4 starting positions (NE, NW, SW, and SE), facing to the pool wall. They were then required to swim to find the hidden platform (13 cm in diameter, located in the SW quadrant), which was submerged 1 cm under water. During each trial, mice were allowed to swim until they found the hidden platform where they remained for 20 seconds before being returned to a holding cage. Mice that failed to find the hidden platform in 120 seconds were guided to the platform where they remained for 20 seconds. Twenty-four hours after the final training trial, mice were returned to the pool from a novel drop point with the hidden platform absent for 120 seconds, and their swim path was recorded.

Electrophysiological recordings in freely moving rat

Electrodes implantation. One hundred rats were chronically implanted with electrodes as described previously (20, 21), and 12 animals were exclude from the experiment due to nonfunctional electrodes or postoperative complications. Briefly, rats were deeply anesthetized with sodium pentobarbital (60 mg/kg, i.p.) and pretreated with atropine (0.4 mg/kg, i.p.) to prevent excessive salivation. The core temperature of anesthetized rats was maintained at 36.5°C ± 0.5°C. Three stainless steel bone anchor screws (Stoelting Co.) were inserted into the skull by drilled holes without piercing the dura. One screw served as a ground electrode (7 mm posterior to bregma and 5 mm left of the midline), another screw acted as an anchor (opposite the ground screw, 7 mm posterior to bregma and 5 mm right of the midline), and the third screw served as a reference electrode (8 mm anterior to bregma and 1 mm left of the midline). The stimulating electrode was made by gluing together a pair of twisted Teflon-coated 90% platinum/10% iridium wires (50 μm inner diameter, 100 μm outer diameter, A-M Systems Inc.). The recording electrode was a single Teflon-coated platinum iridium wire (75 μm inner diameter, 140 μm outer diameter, A-M Systems Inc.). The recording electrode was lowered into the CA1 pyramidal cell dendritic layer (AP, –3.5 mm; ML, 2.5 mm; DV, ~2.5 mm from skull surface of the dura), and the stimulating electrode was placed in the Schaffer collateral/commissural pathways of the dorsal hippocampus (AP, –4.5 mm; ML, 3.5 mm; DV, ~2.8 mm from skull surface of the dura) via holes drilled through the skull. The electrode socket assembly was fixed onto the skull with dental cement. The correct placement of the electrodes in the CA1 region of the dorsal hippocampus was verified by electrophysiological criteria and postmortem examination.

Electrophysiological recordings in freely moving rats. All rats were allowed to recover for at least 7 days before freely moving recordings were performed. During this recovery period, rats were allowed to acclimatize to the recording chamber (40 × 40 × 60 cm), which was made of black Plexiglas and open at the top, for at least 1 hour each day. To allow rats to move around freely in the chamber during recording, implanted electrodes were connected by a flexible cable and a swivel commutator (Crist Instrument Co. Inc.) to the stimulation and recording equipment. fEPSPs were evoked by square-wave stimulations (pulse width = 0.12 ms). Test fEPSPs were evoked at a frequency of 0.033 Hz and at a stimulus intensity adjusted to around 50% of the maximal response size. After a 30-minute stable baseline, LTP was induced. In the present experiment, 2 high-frequency stimulation protocols were used to induce LTP. To induce an unsaturated form of

LTP that contains only decaying LTP (lasts for less than 1.5 hours), a wHFS that contains 2 trains of 30 pulses at 100 Hz were given, with an intertrain interval of 5 minutes. To induce the stable (nondecaying LTP [over 24 hours], a sHFS that contains 4 trains of 30 pulses at 100 Hz were given, with an intertrain interval of 5 minutes.

Electrophysiological recordings in anesthetized transgenic mice

Mice were deeply anesthetized with sodium pentobarbital at a dose of 60 mg/kg (i.p.) within their home cages and then mounted to a stereotaxic frame (Stoelting Co.). The core temperature was monitored and kept at 36.5°C ± 0.5°C. Two electrodes (a pair of 100 μm outer diameter Teflon-coated wires; A-M Systems Inc.) were slowly inserted into the brain through drilled holes. A stimulating electrode was placed at the Schaffer collaterals of dorsal hippocampus (AP, –1.7–1.9 mm; ML, 1.7–1.9 mm; DV, 1.6–2.0 mm from skull surface of the dura), and a recording electrode was placed at the ipsilateral striatum radiatum of hippocampal CA1 area (AP, –1.7–1.9 mm; ML, 1.2–1.3 mm; DV, 1.5–1.9 mm from skull surface of the dura). Placements of the 2 electrodes were slowly adjusted to obtain the optimal response of EPSP. Electrophysiological signals were recorded with an extracellular amplifier (model 3600) and SciWorks data acquisition system provided by A-M Systems. Stimulating pulses (100-μs duration), with an intensity that evoked one-half of maximum amplitude, were delivered at 0.033 Hz to obtain a stable baseline for at least 30 minutes. Once a stable baseline was established, a sHFS that contains 4 trains of 30 pulses at 100 Hz, with an intertrain interval of 5 minutes, was delivered to induce LTP. The correct placement of the electrodes in the CA1 region of the dorsal hippocampus was verified by electrophysiological criteria and postmortem examination.

Immunohistochemistry

Mice were euthanized after behavioral testing, and one-half of the brains was immediately frozen for protein extraction. The other half of the brains was fixed in freshly depolymerized 4% paraformaldehyde and sectioned with a Cryostat (Leica) to 30-μm thickness for immunocytochemical staining as previously described (36, 37). Every sixth slice with the same reference position was mounted onto slides for staining. Immunocytochemical staining was performed on floating sections. The slices were immunostained with biotinylated monoclonal 4G8 antibody at 1:500 dilution. Plaques were visualized by the ABC and DAB method and counted by microscopy at ×40 magnification. Plaques were quantitated, and the mean plaque count per slice was recorded for each mouse.

Western blotting

Subcellular fractionation. After behavioral testing, the hippocampal tissue from rats and transgenic mice was collected for Western blotting. The tissue was homogenized in ice-cold Tris-HCl buffer (30 mM, pH 7.4) containing 4 mM EDTA, 1 mM EGTA, 100 μM $(NH_4)_6Mo_7O_{24}$, 5 mM $Na_4P_2O_7$, 25 mM NaF, 1 mM Na_3VO_4, and a cocktail of protease inhibitors (Complete, Roche). Subcellular fractions were prepared as previously described (26). Briefly, the hippocampal homogenates were centrifuged twice at 4°C at 700 *g* for 7 minutes to remove nuclei and other debris. The 2 supernatants were pooled and centrifuged at 100,000 *g* at 4°C for 60 minutes. Pellets were resuspended in the same buffer containing 0.5% Tri-

ton X-100 and incubated at 4°C for 20 minutes, layered over 1 M sucrose, and centrifuged at 100,000 *g* for 60 minutes. Finally, the Triton-insoluble material that sedimented through the sucrose layer, which is highly enriched in postsynaptic densities, was resuspended in the same buffer containing 1% SDS and stored at −80°C. Total protein concentration was determined by the BCA Protein Assay Kit (Pierce).

Immunoblotting. Samples were aliquoted such that they were in uniform amounts (30 μg for total protein and 10 μg for subcellular fraction) and boiled with 4X sample buffer at 95°C for 5 minutes. The samples were then separated on 10% SDS-PAGE gels and transferred onto polyvinylidenedifluoride membranes. To block nonspecific background, the membranes were incubated with 5% fat-free milk for 1 hour at room temperature. The target proteins were immunoblotted with primary antibody overnight at 4°C to GluA1 (1:3,000), GluA2 (1:1,000), or PKMζ (1:4,000), followed by incubation with HRP-conjugated secondary antibody (1:3,000, 1 hour at room temperature). For sequential blotting, the membranes were stripped with stripping buffer and probed with a second antibody. The blots were developed by the Enhanced Chemiluminescence Detection System (Amersham ECL) and imaged by the Bio-Rad ChemiDoc XRS+ system. The intensities of bands of interest (raw data) were quantified using Bio-Rad Quantity One software. The relative level of target protein is expressed as the percentage difference of the intensity of the target protein and the marker protein, such as postsynaptic marker PSD-95 (1:500) and cytoplasmic marker β-actin (1:5,000).

Statistics

All results are presented as mean ± SEM and were analyzed by ANOVA or 2-tailed Student's *t* test. Statistical significance was accepted at $P < 0.05$.

Study approval

All experimental protocols were approved by the University of British Columbia Animal Care Committee and the Chongqing Medical University Animal Care Committee. All efforts were made to minimize animal suffering and to reduce the number of animals used.

Address correspondence to: Zhifang Dong, 136 Zhongshan Er Road, Yuzhong District, Chongqing 400014, PR China. Phone: 0086.23.63637857; E-mail: zfdong@cqmu.edu.cn. Or to: Tingyu Li, 136 Zhongshan Er Road, Yuzhong District, Chongqing 400014, PR China. Phone: 0086.23.63630913; E-mail: tyli@vip.sina.com. Or to: Weihong Song, 2255 Wesbrook Mall, Vancouver, British Columbia V6T 1Z3, Canada. Phone: 604.822.8019; E-mail: weihong@mail.ubc.ca. Or to: Yu Tian Wang, F117-2211 Wesbrook Mall, Vancouver, BC V6T 2B5, Canada. Phone: 604.822.0398; E-mail: ytwang@brain.ubc.ca.

1. Bliss TV, Collingridge GL. A synaptic model of memory: long-term potentiation in the hippocampus. *Nature*. 1993;361(6407):31–39.
2. Collingridge GL, Isaac JT, Wang YT. Receptor trafficking and synaptic plasticity. *Nat Rev Neurosci*. 2004;5(12):952–962.
3. Frey U, Morris RG. Synaptic tagging: implications for late maintenance of hippocampal long-term potentiation. *Trends Neurosci*. 1998;21(5):181–188.
4. Malenka RC, Nicoll RA. Long-term potentiation--a decade of progress? *Science*. 1999;285(5435):1870–1874.
5. Sacktor TC. PKMzeta, LTP maintenance, and the dynamic molecular biology of memory storage. *Prog Brain Res*. 2008;169:27–40.
6. Abel T, Nguyen PV, Barad M, Deuel TA, Kandel ER, Bourtchouladze R. Genetic demonstration of a role for PKA in the late phase of LTP and in hippocampus-based long-term memory. *Cell*. 1997;88(5):615–626.
7. Pastalkova E, Serrano P, Pinkhasova D, Wallace E, Fenton AA, Sacktor TC. Storage of spatial information by the maintenance mechanism of LTP. *Science*. 2006;313(5790):1141–1144.
8. Frey U, Huang YY, Kandel ER. Effects of cAMP simulate a late stage of LTP in hippocampal CA1 neurons. *Science*. 1993;260(5114):1661–1664.
9. Huang EP. Synaptic plasticity: going through phases with LTP. *Curr Biol*. 1998;8(10):R350–R352.
10. Frey U, Krug M, Reymann KG, Matthies H. Anisomycin, an inhibitor of protein synthesis, blocks late phases of LTP phenomena in the hippocampal CA1 region in vitro. *Brain Res*. 1988;452(1):57–65.
11. Krug M, Lossner B, Ott T. Anisomycin blocks the late phase of long-term potentiation in the dentate gyrus of freely moving rats. *Brain Res Bull*. 1984;13(1):39–42.
12. Muller D, Nikonenko I, Jourdain P, Alberi S. LTP, memory and structural plasticity. *Curr Mol Med*. 2002;2(7):605–611.
13. Nguyen PV, Abel T, Kandel ER. Requirement of a critical period of transcription for induction of a late phase of LTP. *Science*. 1994;265(5175):1104–1107.
14. Davis HP, Squire LR. Protein synthesis and memory: a review. *Psychol Bull*. 1984;96(3):518–559.
15. Lu Y, et al. TrkB as a potential synaptic and behavioral tag. *J Neurosci*. 2011;31(33):11762–11771.
16. Villarreal DM, Do V, Haddad E, Derrick BE. NMDA receptor antagonists sustain LTP and spatial memory: active processes mediate LTP decay. *Nat Neurosci*. 2002;5(1):48–52.
17. Xiao MY, Niu YP, Wigstrom H. Activity-dependent decay of early LTP revealed by dual EPSP recording in hippocampal slices from young rats. *Eur J Neurosci*. 1996;8(9):1916–1923.
18. Bartlett TE, Wang YT. Illuminating synapse-specific homeostatic plasticity. *Neuron*. 2011;72(5):682–685.
19. Hou Q, Gilbert J, Man HY. Homeostatic regulation of AMPA receptor trafficking and degradation by light-controlled single-synaptic activation. *Neuron*. 2011;72(5):806–818.
20. Dong Z, et al. Mechanisms of hippocampal long-term depression are required for memory enhancement by novelty exploration. *J Neurosci*. 2012;32(35):11980–11990.
21. Ge Y, et al. Hippocampal long-term depression is required for the consolidation of spatial memory. *Proc Natl Acad Sci U S A*. 2010;107(38):16697–16702.
22. Yang K, Xiong W, Yang G, Kojic L, Wang YT, Cynader M. The regulatory role of long-term depression in juvenile and adult mouse ocular dominance plasticity. *Sci Rep*. 2012;1:203.
23. Ahmadian G, et al. Tyrosine phosphorylation of GluR2 is required for insulin-stimulated AMPA receptor endocytosis and LTD. *EMBO J*. 2004;23(5):1040–1050.
24. Brebner K, et al. Nucleus accumbens long-term depression and the expression of behavioral sensitization. *Science*. 2005;310(5752):1340–1343.
25. Van den Oever MC, et al. Prefrontal cortex AMPA receptor plasticity is crucial for cue-induced relapse to heroin-seeking. *Nat Neurosci*. 2008;11(9):1053–1058.
26. Migues PV, et al. PKMzeta maintains memories

by regulating GluR2-dependent AMPA receptor trafficking. *Nat Neurosci*. 2010;13(5):630–634.

27. Yao Y, et al. PKM zeta maintains late long-term potentiation by N-ethylmaleimide-sensitive factor/GluR2-dependent trafficking of postsynaptic AMPA receptors. *J Neurosci*. 2008;28(31):7820–7827.

28. Sacktor TC. How does PKMzeta maintain long-term memory? *Nat Rev Neurosci*. 2011;12(1):9–15.

29. Frankland PW, Josselyn SA. Neuroscience: Memory and the single molecule. *Nature*. 2013;493(7432):312–313.

30. Lee AM, et al. Prkcz null mice show normal learning and memory. *Nature*. 2013;493(7432):416–419.

31. Volk LJ, Bachman JL, Johnson R, Yu Y, Huganir RL. PKM-zeta is not required for hippocampal synaptic plasticity, learning and memory. *Nature*. 2013;493(7432):420–423.

32. Marchetti C, Marie H. Hippocampal synaptic plasticity in Alzheimer's disease: what have we learned so far from transgenic models? *Rev Neurosci*. 2011;22(4):373–402.

33. Rowan MJ, Klyubin I, Cullen WK, Anwyl R. Synaptic plasticity in animal models of early Alzheimer's disease. *Philos Trans R Soc Lond B Biol Sci*. 2003;358(1432):821–828.

34. Crary JF, Shao CY, Mirra SS, Hernandez AI, Sacktor TC. Atypical protein kinase C in neurodegenerative disease I: PKMzeta aggregates with limbic neurofibrillary tangles and AMPA receptors in Alzheimer disease. *J Neuropathol Exp Neurol*. 2006;65(4):319–326.

35. Shao CY, Mirra SS, Sait HB, Sacktor TC, Sigurdsson EM. Postsynaptic degeneration as revealed by PSD-95 reduction occurs after advanced Abeta and tau pathology in transgenic mouse models of Alzheimer's disease. *Acta Neuropathol*. 2011;122(3):285–292.

36. Qing H, et al. Valproic acid inhibits Abeta production, neuritic plaque formation, and behavioral deficits in Alzheimer's disease mouse models. *J Exp Med*. 2008;205(12):2781–2789.

37. Ly PT, et al. Inhibition of GSK3beta-mediated BACE1 expression reduces Alzheimer-associated phenotypes. *J Clin Invest*. 2013;123(1):224–235.

38. Harris ME, Hensley K, Butterfield DA, Leedle RA, Carney JM. Direct evidence of oxidative injury produced by the Alzheimer's beta-amyloid peptide (1-40) in cultured hippocampal neurons. *Exp Neurol*. 1995;131(2):193–202.

39. Markesbery WR. The role of oxidative stress in Alzheimer disease. *Arch Neurol*. 1999;56(12):1449–1452.

40. Mattson MP, Cheng B, Davis D, Bryant K, Lieberburg I, Rydel RE. beta-Amyloid peptides destabilize calcium homeostasis and render human cortical neurons vulnerable to excitotoxicity. *J Neurosci*. 1992;12(2):376–389.

41. Gu X, Sun J, Li S, Wu X, Li L. Oxidative stress induces DNA demethylation and histone acetylation in SH-SY5Y cells: potential epigenetic mechanisms in gene transcription in Abeta production. *Neurobiol Aging*. 2013;34(4):1069–1079.

42. Wang Y, et al. alpha-Amino-3-hydroxy-5-methyli-soxazole-4-propionic acid subtype glutamate receptor (AMPAR) endocytosis is essential for N-methyl-D-aspartate-induced neuronal apoptosis. *J Biol Chem*. 2004;279(40):41267–41270.

43. Hsieh H, et al. AMPAR removal underlies Abeta-induced synaptic depression and dendritic spine loss. *Neuron*. 2006;52(5):831–843.

44. Ren SQ, et al. PKClambda is critical in AMPA receptor phosphorylation and synaptic incorporation during LTP. *EMBO J*. 2013;32(10):1365–1380.

45. Malinow R, Malenka RC. AMPA receptor trafficking and synaptic plasticity. *Annu Rev Neurosci*. 2002;25:103–126.

46. Mitsushima D, Ishihara K, Sano A, Kessels HW, Takahashi T. Contextual learning requires synaptic AMPA receptor delivery in the hippocampus. *Proc Natl Acad Sci U S A*. 2011;108(30):12503–12508.

47. Whitlock JR, Heynen AJ, Shuler MG, Bear MF. Learning induces long-term potentiation in the hippocampus. *Science*. 2006;313(5790):1093–1097.

48. Plant K, et al. Transient incorporation of native GluR2-lacking AMPA receptors during hippocampal long-term potentiation. *Nat Neurosci*. 2006;9(5):602–604.

49. Li Z, et al. Caspase-3 activation via mitochondria is required for long-term depression and AMPA receptor internalization. *Cell*. 2010;141(5):859–871.

50. Zhang YH, Kays J, Hodgdon KE, Sacktor TC, Nicol GD. Nerve growth factor enhances the excitability of rat sensory neurons through activation of the atypical protein kinase C isoform, PKMzeta. *J Neurophysiol*. 2012;107(1):315–335.